

Optofluidic 1x4 switch

Alex Groisman,^{1,*} Steve Zamek,² Kyle Campbell,¹ Lin Pang,² Uriel Levy,^{2,3} and Yeshaiah Fainman^{2,*}

¹Department of Physics, University of California, San Diego, 9500 Gilman Drive, La Jolla, CA 92093-0374

²Department of Electrical and Computer Engineering, University of California, San Diego, 9500 Gilman Drive, La Jolla, CA 92093-0407

³Present address: Dept. of Applied Physics, Hebrew University of Jerusalem, Jerusalem, 91904, Israel.

* Corresponding authors: fainman@ece.ucsd.edu and agroisman@ucsd.edu

Abstract: An optofluidic 1x4 switch is designed, fabricated, and tested. The switch is based on a blazed diffraction grating imprinted onto silicone elastomer at the bottom of a microfluidic channel that is filled with liquids with different refractive indices. When the condition of a diffraction maximum is met, the laser beam incident on the grating is deflected by an angle proportional to the refractive index mismatch between the elastomer and the liquid in the channel. The switch was tested using four different aqueous salt solutions generating 0th to 3rd orders of diffraction. The insertion loss was <2.5dB, the extinction ratio was >9.8dB, and the response time was 55 ms. The same basic design can be used to build optofluidic switches with more than 4 outputs.

© 2008 Optical Society of America

OCIS codes: (050.1950) Diffraction gratings; (130.4815); Optical switching devices; (220.4880) Optomechanics.

References and links

1. G. M. Whitesides, "The origins and the future of microfluidics," *Nature* **442**, 368-373 (2006).
2. G. H. W. Sanders and A. Manz, "Chip-based microsystems for genomic and proteomic analysis," *TrAC-Trends Anal. Chem.* **19**, 364-378 (2000).
3. D. J. Beebe, G. A. Mensing, and G. M. Walker, "Physics and applications of microfluidics in biology," *Annu. Rev. Biomed. Eng.* **4**, 261-286 (2002).
4. T. M. Squires, and S. R. Quake, "Microfluidics: Fluid physics at the nanoliter scale," *Rev. Mod. Phys.* **77**, 977-1026 (2005).
5. M. Toner and D. Irimia, "Blood-on-a-chip," *Annu. Rev. Biomed. Eng.* **7**, 77-103 (2005).
6. A. Khademhosseini, R. Langer, J. Borenstein, and J. P. Vacanti, "Microscale technologies for tissue engineering and biology," *Proceedings of the National Academy of Sciences of the United States of America* **103**, 2480-2487 (2006).
7. D. Psaltis, S. R. Quake, and C. H. Yang, "Developing optofluidic technology through the fusion of microfluidics and optics," *Nature* **442**, 381-386 (2006).
8. C. Monat, P. Domachuk, and B. J. Eggleton, "Integrated optofluidics: A new river of light," *Nat. Photonics* **1**, 106-114 (2007).
9. U. Levy and R. Shamai, "Tunable optofluidic devices," *Microfluid. Nanofluid.* **4**, 97-105 (2008).
10. N. Chronis, G. L. Liu, K. H. Jeong, and L. P. Lee, "Tunable liquid-filled microlens array integrated with microfluidic network," *Opt. Express* **11**, 2370-2378 (2003).
11. D. B. Wolfe, D. V. Vezenov, B. T. Mayers, G. M. Whitesides, R. S. Conroy, and M. G. Prentiss, "Diffusion-controlled optical elements for optofluidics," *Appl. Phys. Lett.* **87** (2005).
12. L. Diehl, B. G. Lee, P. Behroozi, M. Loncar, M. A. Belkin, F. Capasso, T. Aellen, D. Hofstetter, M. Beck, and J. Faist, "Microfluidic tuning of distributed feedback quantum cascade lasers," *Opt. Express* **14**, 11660-11667 (2006).
13. D. Erickson, T. Rockwood, T. Emery, A. Scherer, and D. Psaltis, "Nanofluidic tuning of photonic crystal circuits," *Opt. Lett.* **31**, 59-61 (2006).
14. M. Gersborg-Hansen, and A. Kristensen, "Optofluidic third order distributed feedback dye laser," *Appl. Phys. Lett.* **89** (2006).
15. Z. Y. Li, Z. Y. Zhang, A. Scherer, and D. Psaltis, "Mechanically tunable optofluidic distributed feedback dye laser," *Opt. Express* **14**, 10494-10499 (2006).
16. M. Loncar, B. G. Lee, L. Diehl, M. Belkin, F. Capasso, M. Giovannini, J. Faist, and E. Gini, "Design and fabrication of photonic crystal quantum cascade lasers for optofluidics," *Opt. Express* **15**, 4499-4514 (2007).

17. L. Pang, U. Levy, K. Campbell, A. Groisman, and Y. Fainman, "Set of two orthogonal adaptive cylindrical lenses in a monolith elastomer device," *Opt. Express* **13**, 9003-9013 (2005).
 18. K. Campbell, A. Groisman, U. Levy, L. Pang, S. Mookherjee, D. Psaltis, and Y. Fainman, "A microfluidic 2x2 optical switch," *Appl. Phys. Lett.* **85**, 6119-6121 (2004).
 19. R. A. Soref, "Liquid-Crystal Fiberoptic Switch," *Opt. Lett.* **4**, 155-157 (1979).
 20. M. Kobayashi, H. Terui, M. Kawachi, and J. Noda, "2x2 Optical-Waveguide Matrix Switch Using Nematic Liquid-Crystal," *IEEE J. Quantum Electron.* **18**, 1603-1610 (1982).
 21. D. A. B. Miller, D. S. Chemla, T. C. Damen, A. C. Gossard, W. Wiegmann, T. H. Wood, and C. A. Burrus, "Novel Hybrid Optically Bistable Switch - The Quantum Well Self-Electro-Optic Effect Device," *Appl. Phys. Lett.* **45**, 13-15 (1984).
 22. S. K. Korotky, G. Eisenstein, R. S. Tucker, J. J. Veselka, and G. Raybon, "Optical-Intensity Modulation To 40 Ghz Using A Wave-Guide Electrooptic Switch," *Appl. Phys. Lett.* **50**, 1631-1633 (1987).
 23. D. A. Smith, R. S. Chakravarthy, Z. Y. Bao, J. E. Baran, J. L. Jackel, A. d'Alessandro, D. J. Fritz, S. H. Huang, X. Y. Zou, S. M. Hwang, A. E. Willner, and K. D. Li, "Evolution of the acousto-optic wavelength routing switch," *J. Lightwave Technol.* **14**, 1005-1019 (1996).
 24. E. A. Camargo, H. M. H. Chong, and R. M. De la Rue, "2D Photonic crystal thermo-optic switch based on AlGaAs/GaAs epitaxial structure," *Opt. Express* **12**, 588-592 (2004).
 25. M. Shirasaki, H. Takamatsu, and T. Obokata, "Bistable Magneto-Optic Switch For Multimode Optical Fiber," *Appl. Opt.* **21**, 1943-1949 (1982).
 26. V. Studer, G. Hang, A. Pandolfi, M. Ortiz, W. F. Anderson, and S. R. Quake, "Scaling properties of a low-actuation pressure microfluidic valve," *J. Appl. Phys.* **95**, 393-398 (2004).
 27. M. G. Moharam, and T. K. Gaylord, "Diffraction Analysis Of Dielectric Surface-Relief Gratings," *J. Opt. Soc. Am.* **72**, 1385-1392 (1982).
 28. S. T. Peng, T. Tamir, and H. L. Bertoni, "Theory Of Periodic Dielectric Waveguides," *IEEE Trans. Microwave Theory Tech.* **MT23**, 123-133 (1975).
-

1. Introduction

Microfluidics is a quickly growing area of applied science and technology with numerous applications in biology, chemistry, biochemistry, and medicine[1-6]. During the last decade, the complexity, levels of integration, and miniaturization of microfluidic networks have been steadily increasing. Nevertheless, imaging and optical interrogation of microchannels have usually been performed with conventional free-space optics built of components much larger than the microchannels themselves. Integration of microfluidic and optical components into a single miniaturized platform is one of the goals of optofluidics[7-9]. This integration requires the development of new types of miniature lenses, waveguides, switches, sources, filters, and detectors that can be effectively combined with microfluidic networks.

Some of these optical components can be built of microchannels themselves and can be adjusted by changing the shapes of the microchannels and refractive indices of liquids in them[10-17]. In addition to the optofluidic integration, adaptive optical devices made with microfluidic technology can also be used as stand-alone optical elements. One such device is a recently introduced 2x2 optofluidic switch[18] that employs the effect of total internal reflection and is made of polydimethylsiloxane (PDMS), an inexpensive, optically clear and chemically inert silicone elastomer. The main functional element of the switch is a flat-parallel microchannel that acts as either a mirror or a transparent window, when it is filled with a low refractive index liquid or an index-matching solution, respectively. The optofluidic switch can be integrated with microfluidic networks and serve as an alternative to the existing optical switches that use liquid crystals [19, 20] or electro-optic[21, 22], acousto-optic[23], thermo-optic[24], or magneto-optic effects[25].

In this paper we introduce 1xN optofluidic switches, which are based on diffraction rather than reflection, and describe the design and operation of a 1x4 switch that we built and tested. The main functional element of the proposed 1xN switches is a blazed diffraction grating imprinted onto the bottom of a microfluidic channel [Fig. 1(a)]. A collimated monochromatic beam of light incident onto the grating is deflected by an angle that is proportional to the mismatch between the refractive indices of the material of the grating and the liquid in the channel [Fig. 1(b)]. For a given wavelength of light, diffraction maxima occur at a discrete set of refractive indices of the liquid that correspond to a discrete set of beam deflection angles, making a 1xN optical switch.

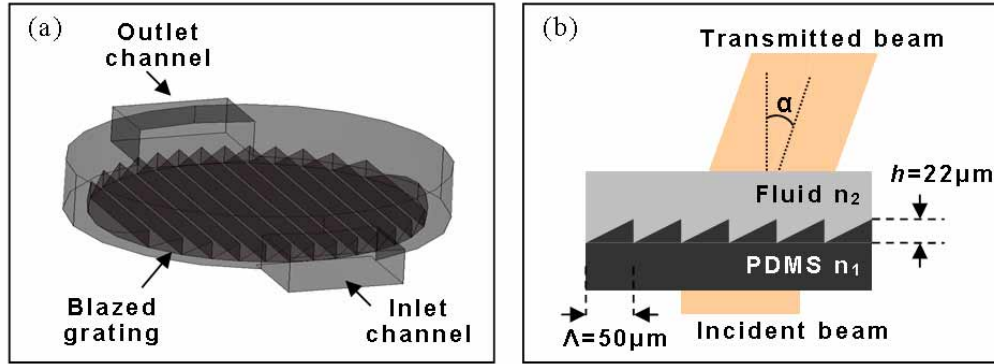


Fig. 1. The optofluidic switch. (a) The functional area of the device (diffraction channel), consisting of a circular microchannel with a blazed grating imprinted onto its bottom. (b) Schematic drawing of the blazed grating with the incident and transmitted laser beams.

2. Design and operation of the optofluidic switch.

Within each period (segment) of an ideal thin blazed grating, the phase of an incident monochromatic wave is linearly modulated in the transverse plane along the direction perpendicular to the grooves of the grating (Fig. 1). The slope of this linear modulation is proportional to the difference between the refractive indices of the material of the grating, n_1 , and of the medium on top of the grating, n_2 . A diffraction maximum occurs when the optical path difference over one period of the blazed profile is equal to an integer number of wavelengths:

$$(n_1 - n_2)h = \lambda m, \quad (1)$$

where h is the height of the grating profile, λ is the wavelength of the incident light in vacuum, and m is an integer indicating the order of diffraction. When the condition of a diffraction maximum is met, a normally incident plane wave is coherently deflected by an angle α_m found from the equation

$$\sin(\alpha_m) = \lambda m / \Lambda = (n_1 - n_2)h / \Lambda \quad (2)$$

where Λ is the period of the grating. At a diffraction maximum, an ideal blazed grating acts as a prism with an angle $\tan^{-1}(h/\Lambda)$.

The blazed grating at the bottom of the microchannel [Fig. 1(b)] was made of PDMS with a refractive index $n_1 \approx 1.41$ and had $\Lambda = 50 \mu\text{m}$ and $h = 22.5 \mu\text{m}$. The working liquids fed into the microchannel were four different solutions of KI and NaBr in water, all containing 2 parts of KI and 1 part of NaBr (by weight), but having different total concentrations of the two salts. The refractive indices of the solutions, n_2 , varied between $n_1 \approx 1.41$ (~40% of total KI and NaBr) and 1.34 (~5% of total KI and NaBr). According to Eqs. (1) and (2), for a light beam with $\lambda = 532 \text{ nm}$, there are 4 separate maxima of diffraction in this range of n_2 , with $m = 0 - 3$ and with the deflection angles varying by 0.6° from 0 to 1.8° .

The microfluidic device consisted of a PDMS chip bonded to a #1.5 microscope cover glass (Fig. 2). The chip was assembled of two layers of PDMS and had two layers of microchannels, a flow layer (in the first layer of PDMS) and a control layer (in the second layer of PDMS). The control layer had 5 separate inlets [c0 – c4 in Fig. 2(a)] connected to 6 “push-up” membrane valves[26] and consisted of $40 \mu\text{m}$ deep channels with rectangular profiles. When a control layer inlet was pressurized, membrane valves [blue rectangles in Fig. 2(a)] connected to the inlet were actuated and locally sealed flow channels above the valves [red segments in Fig. 2(a)]. The flow layer had 4 inlets [in0 – in3 in Fig. 2(a), for KI-NaBr

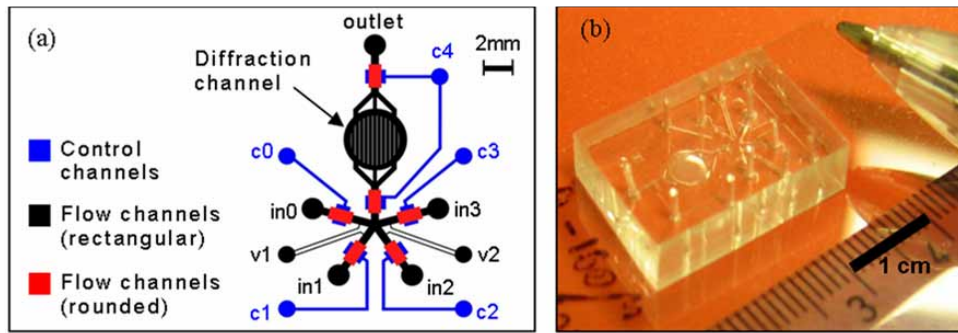


Fig. 2. Optofluidic switch. (a) Layout of microchannels in the device: the flow layer (black and red) with four inlets (in0 – in3), two vents (v1 and v2), and one outlet; the control layer (blue) with 5 inlets (c0 – c4). The blazed grating is schematically shown as a patterned area. (b) A photograph of an actual microfluidic PDMS chip bonded to a cover glass.

solutions with different refractive indices], one outlet, and two vents [v1 and v2 in Fig. 2(a)]. Microchannels in the flow layer had rectangular profiles and a depth of 180 μm [shown in black in Fig. 2(a)], except for the segments on top of the membrane valves [shown in red in Fig. 2(a)] that had rounded profiles and a depth of 100 μm . The blazed grating had a circular footprint, ~ 3.5 mm in diameter, and was situated in the middle of the bottom of a circular microchannel (diffraction channel) that was 4.5 mm in diameter.

3. Fabrication protocol.

Each of the two layers of PDMS (Sylgard 184 by Dow Corning) comprising the microfluidic chip was cast using a dedicated master mold, a silicon wafer with a lithographically fabricated micro-relief (Fig. 3). Both molds had relief features for 12 separate devices. Fabrication of the blazed diffraction gratings, which were imprinted onto the upper surface of the second layer of PDMS [Fig. 3(b)], was done using specially made stamps that were ~ 3.5 mm in diameter, ~ 5 mm tall cylindrical pieces of PDMS with the blazed grating relief engraved on their bases. To make the stamps, a 5 mm thick PDMS replica of a commercial blazed grating (253-*940R by Newport) was cast and subsequently punched using a sharpened steel tube with an inner diameter of ~ 4 mm. The stamps were further treated with trichloromethylsilane (TMCS) to make their surface non-sticky.

Because the first (upper) layer of PDMS had microchannels of two kinds [rectangular and rounded flow channels in Fig. 2(a)], the fabrication of the master mold for the first layer required two steps of photolithography. A 5" silicon wafer was first coated with a 180 μm layer of a UV-curable epoxy (SU8 2050 by Microchem), exposed to UV-light through a photomask (photo-plotted film with a resolution of 10,000 dpi), and developed. After that, the wafer was coated with a 100 μm layer of a positive photoresist (AZ-50XT by Clarion), exposed to UV-light through another photomask and developed [Fig. 3(a)]. The wafer was placed into a 110°C convection oven for 20 min, to make the AZ-50XT relief features reflow and acquire rounded shapes, as required for proper operation of the push-up membrane valves. An ~ 5 mm layer of a PDMS pre-polymer (5:1 mixture of base and curing agent) was poured onto the master mold and cured by baking for 45 min in an 80°C oven. The PDMS cast was then peeled off from the wafer, cut into individual chips, and holes were punched in the chips with a gauge 20 luer stub to make the flow layer ports [four inlets, one outlet, and two vents; Fig. 2(a)], completing the first layer of the chips.

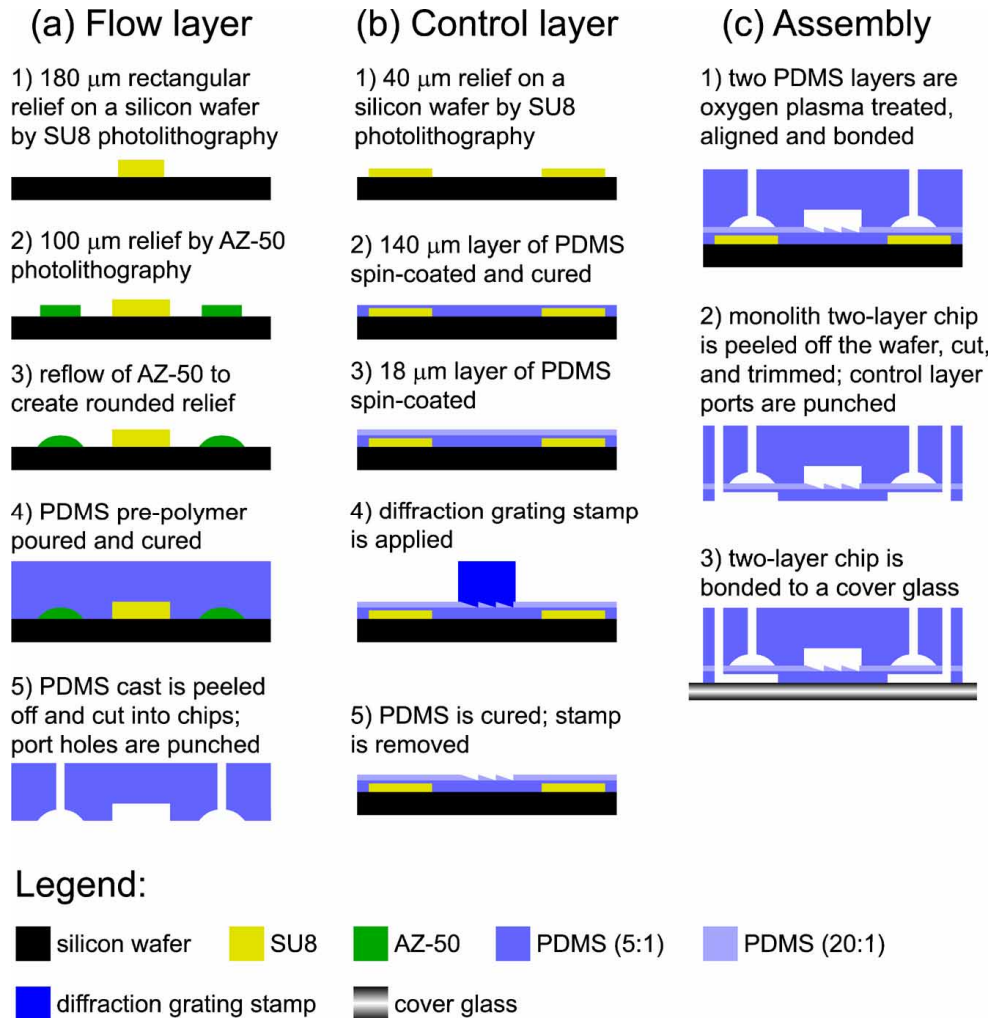


Fig. 3. Fabrication of the optofluidic switch. (a) Fabrication of the first layer of PDMS, step-by-step. (b) Fabrication of the second layer of PDMS with imprinted blazed grating. (c) Assembly of the device.

The master mold for the second (lower) layer of PDMS was fabricated by patterning a 5" silicon wafer with a 40 μm thick layer of SU8 epoxy, exposing it to UV-light through a third photomask, and developing it [Fig. 3(b)]. The mold was spin-coated with a $\sim 140 \mu\text{m}$ layer of the PDMS pre-polymer (5:1 mixture of base and curing agent) that was partially cured and subsequently spin-coated with a $\sim 18 \mu\text{m}$ layer of a differently prepared PDMS pre-polymer (20:1 of base to curing agent). A stamp with engraved diffraction grating was placed on top of the PDMS layer in the middle of the diffraction channel, and the entire structure was baked in the 80 $^{\circ}\text{C}$ oven to completely cure PDMS. (To reduce the adhesion between the stamp and the uncured PDMS, the mold with the uncured PDMS was baked for ~ 2 min in the 80 $^{\circ}\text{C}$ oven prior to the application of the stamp). After the baking, the stamp was separated from the cured PDMS layer, leaving the pattern of a blazed diffraction grating on the PDMS surface.

The first layer PDMS chips were permanently bonded to the cured PDMS on the wafer by using the oxygen plasma treatment [Fig. 3(c)]. The monolith two-layer chips were separated from the wafer, and holes in the chips were punched with a gauge 20 luer stub to produce ports for the control layer [c0 – c4 in Fig. 2(a)]. The microfluidic devices were completed by bonding the two-layer chips to #1.5 microscope cover glasses [Fig. 3(c)].

4. Experimental setup and results

The solutions fed into and drawn off the flow layer of the microfluidic device were kept in 60 cc plastic syringes held upright with their luer connectors at the bottom. The syringes were connected to the ports of the device through luer stubs, lines of flexible Tygon tubing with an inner diameter of 1 mm, and short segments of hypodermic tubing that were inserted into the ports. The syringes connected to the outlet and to the vents (v1 and v2) were filled with water and were open to the atmosphere at the top. The syringes feeding the inlets were connected at the top to a regulated source of pressurized air, creating a differential pressure $\Delta P = 5.0$ psi between the inlets and the outlet (and between the inlets and the vents) that drove the flow through the device. The syringes connected to inlets in0 – in3 were filled with four different KI-NaBr solutions, whose concentrations were individually adjusted to generate diffraction patterns with maximal power of light in the diffraction orders $m = 0 - 3$, respectively. The adjustment was done by steps of $\sim 1\%$ in the total concentration of KI-NaBr, corresponding to steps of $\sim 2 \times 10^{-3}$ in refractive index. Therefore, the refractive indices of the solutions were expected to deviate from their optimal values by $< 1 \times 10^{-3}$, which was $\sim 4\%$ of the difference of 0.023 between refractive indices producing consecutive maxima of diffraction according to Eq. (1). The 0th order of diffraction, corresponding to direct transmission of the incident beam, occurred when the refractive index of the solution in the diffraction channel matched that of the PDMS.

The control layer channels were filled with water, and their five inlets (c0 – c4) were connected to a source of compressed air pressurized at 12 psi through five dedicated 3-way solenoid valves (LHDA by the Lee Company, Westbrook, CT). Normally, all five solenoid valves were powered off, transmitting the pressure of 12 psi to all control channels and to all six membrane valves. This pressure kept the valves closed, so there was no flow through the device. (To prevent flow between the two vents, the pressures at the vents were equilibrated by adjusting the heights of the two syringes connected to the vents.) Therefore, the composition of liquid in the diffraction channel remained the same, as did the deflection angle of the incident beam. Neither electrical power nor liquid was consumed by the switch in this steady state.

In order to switch the deflection angle to, say, the angle of the 2nd order of diffraction, the solenoid valves connected to the control inlets c2 and c4 were simultaneously powered on, venting the two control inlets to the atmosphere and opening the three membrane valves connected to the two control inlets [Fig. 2(a)]. Once the membrane valves opened, the flow from inlet in2 to the outlet started, displacing the liquid in the circular diffraction channel with the solution fed into in2 [Fig. 2(a)]. At the same time, the differential pressure, ΔP , between inlet in2 and the vents generated a flow from the 5-way intersection to the two vents [Fig. 2(a)], purging the dead volumes between the intersection and the closed valves 0, 1, and 3. The flow to the vents prevented contamination of the solution from in2 that was fed to the diffraction channel by the solutions from in0, in1, and in3. The rate of this purging flow was relatively low, because the channels connecting the 5-way intersection with the vents were narrow and had relatively high flow resistances [Fig. 2(a)]. When the solution in the diffraction channel was exchanged, the solenoid valves were powered off again, the membrane valves were closed, and flow through the device was stopped.

The optofluidic switch was tested with a collimated beam, 0.4 mm in diameter, derived from a solid state green laser with a wavelength $\lambda = 532$ nm. The power of the laser (10 mW) was attenuated to 30 μ W. The laser beam was incident at 90° onto the center of the blazed diffraction grating in the functional area of the switch (Fig. 1). To measure the deflection angle of the beam for different states of the switch, the beam was directed onto a distant screen and the separation between the peaks of intensity in different states was measured with a ruler. The angular distance between consecutive peaks was 0.6° in agreement with Eq. (1). To measure the profile of the transmitted laser beam, we used a high speed IEEE 1394 digital camera (Marlin F-033 by Allied Vision Technologies) that worked in a linear regime with a constant gain. The camera had a 640×480 CCD array of 10×10 μ m pixels and was positioned at 140 mm behind the switch on the path of the laser beam. The camera had a full-frame speed

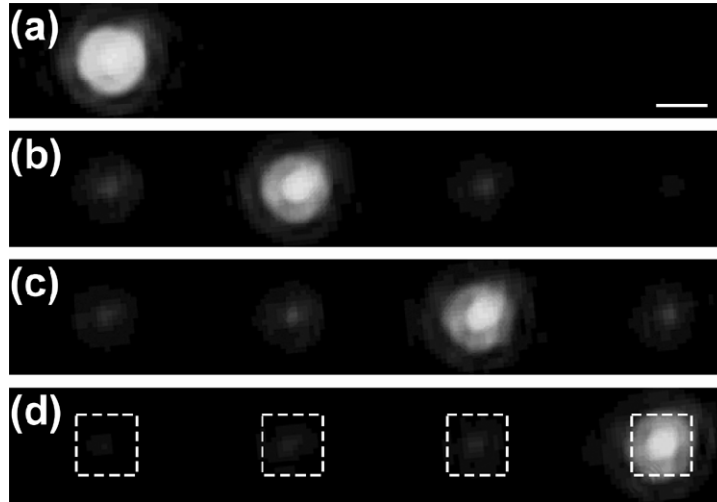


Fig. 4. Transmitted laser light recorded by the CCD camera. (a) – (d) the switch is in the states 0 – 3, respectively. Dashed boxes in (d) indicate zones 0 – 3, from left to right. Scale bar 400 μm .

of 60 frames/sec and was operated at 109 frames/sec with a reduced region of interest. To quantify the power of light propagating along the directions corresponding to the 4 optical outputs of the switch (4 diffraction maxima of the grating), 4 zones (numbered 0 – 3) were selected on the CCD array (Fig. 4). The center of a zone was at the point of highest intensity of the transmitted beam in one of the states of the switch. Each zone was a square $470 \times 470 \mu\text{m}$ (47×47 pixels) in size and subtended an angle of 0.2° (as measured from the blazed grating) that was 3 times smaller than the deflection of the beam between consecutive maxima of diffraction. The power of light directed to a given optical output was measured as the sum of the digitized pixel values from the corresponding zone minus the sum of values of the same pixels when the laser beam was blocked.

Table 1. Power of light (in dB) measured for the 4 optical outputs in the 4 states of the switch, normalized to the power of the 0th output in state 0 of the switch.^a

State of the switch	Power of light by optical outputs (dB)			
	<i>0</i>	<i>1</i>	<i>2</i>	<i>3</i>
0	0	<-24	<-24	<-24
1	-12.9	-1.4	-15.8	<-24
2	-13.3	-11.2	-1.6	-14.2
3	<-24	-19.9	-18.2	-1.7

^a The leftmost column (numbers in bold) indicates the state of the switch and the four columns on the right show the powers of light directed to outputs 0 – 3 (numbers in italic in an upper row) in this state.

Distributions of the power of light in the optical outputs 0 – 3 in the four states of the optofluidic switch are shown in Table 1. In a state m of the switch, the diffraction channel is filled with the solution from the m th inlet, and the m th optical output is intended to be in the ‘ON’ state, with a maximum power of laser light directed to it. In Table 1, the power of light in each optical output is normalized with the power measured in the 0th output in state 0 of the switch (0 dB reference point). In this last state, the light was directly transmitted through the functional region of the switch, and the power of light incident upon the 0th zone was 92%

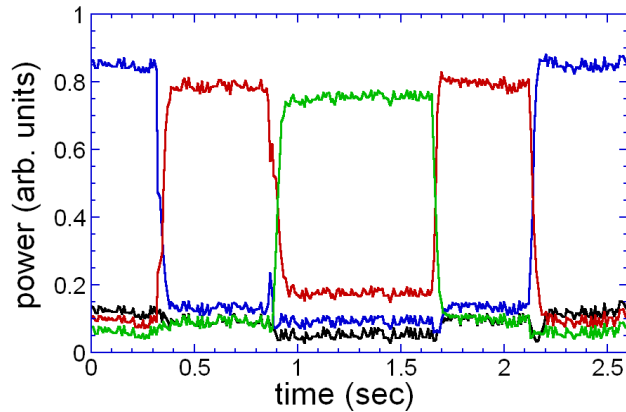


Fig. 5. Powers of laser light (in arbitrary units) directed to outputs 0 – 3 of the switch (measured in zones 0 – 3) as functions of time during a typical series of switching events. Powers in the outputs 0 – 3 are shown in black, blue, red, and green, respectively.

(-0.4 dB) of the total power reaching the CCD array. Compared with state 0, the power of light directed to the optical output intended to be ‘ON’ was reduced in states 1 – 3 by 1.4 – 1.7 dB. Added to the insertion loss of 0.4 dB measured in state 0 (reduction of the total power of the laser light due to the insertion of the device into the light path) and to the 0.4 dB loss due to the limiting of the outputs to the $470 \times 470 \mu\text{m}$ zones, these values amounted to insertion losses of 2.2 to 2.5 dB. The level of cross-talk, the ratio of the powers of light between the optical output that was ‘ON’ and optical outputs that were ‘OFF’ in a given state of the switch, varied from a minimum of -24 dB in state 0 to a maximum of -9.8 dB in state 2. The values of the extinction ratio, the ratio of the light powers directed to a given optical output in the ‘ON’ and ‘OFF’ states of the output, were similar and varied between 24 dB and 9.6 dB (Table 1). The analysis of time series of the powers of light in different zones during switching (Fig. 5) indicated that the transitions between different states of the switch occurred within 55 ms (based on 10% – 90% criterion).

5. Discussion and summary

To evaluate possible factors contributing to the cross-talk between different output channels of the switch, we theoretically analyzed the transmission of a plane wave through the blazed diffraction grating in the functional area of the device. The grating was decomposed into thin layers[27, 28], with each layer treated as a perturbation of the refractive index with the period Λ , and a coupled wave analysis was applied. The optical outputs 0 – 3 of the device were associated with the diffraction orders $m = 0 - 3$ of the grating and with the plane waves propagating at the angles given by Eq. (2). These plane waves became coupled as they propagated through the periodically perturbed dielectric medium that was created by the blazed grating and the liquid above it. The wave propagation was simulated numerically using 31 modes (orders) and 1000 layers. The simulation was performed for refractive indices of the liquid, n_2 , in vicinities of the refractive indices $n_{2,m}$ corresponding to the maxima of diffraction in orders m , as given by Eq. (1) ($n_{2,m} = n_1 - \lambda m / h$). The powers of light directed to the optical outputs 0 – 3 were plotted as functions of $\Delta n = n_2 - n_{2,m}$ (lines in Fig. 6). In addition, finite element method (FEM) was applied to rigorously simulate propagation of the TE mode (symbols in Fig. 6). The discrepancies between the two analyses at small Δn are due to poorly scaled transmission matrices in the coupled wave analysis.

According to the numerical simulations (Fig. 6), the theoretical limit for the cross-talk between different optical outputs of the switch is at -25 dB. One of the possible reasons for

the substantially higher levels of cross-talk observed in the experiments (-10 dB) are large mismatches in the refractive indices, $\Delta n = n_2 - n_{2,m}$. Nevertheless, during the adjustment of the refractive indices of the salt solutions fed into the device inlets, the refractive indices, n_2 , were varied with a step of $\sim 2 \times 10^{-3}$ until a minimum of the cross-talk was found. For a

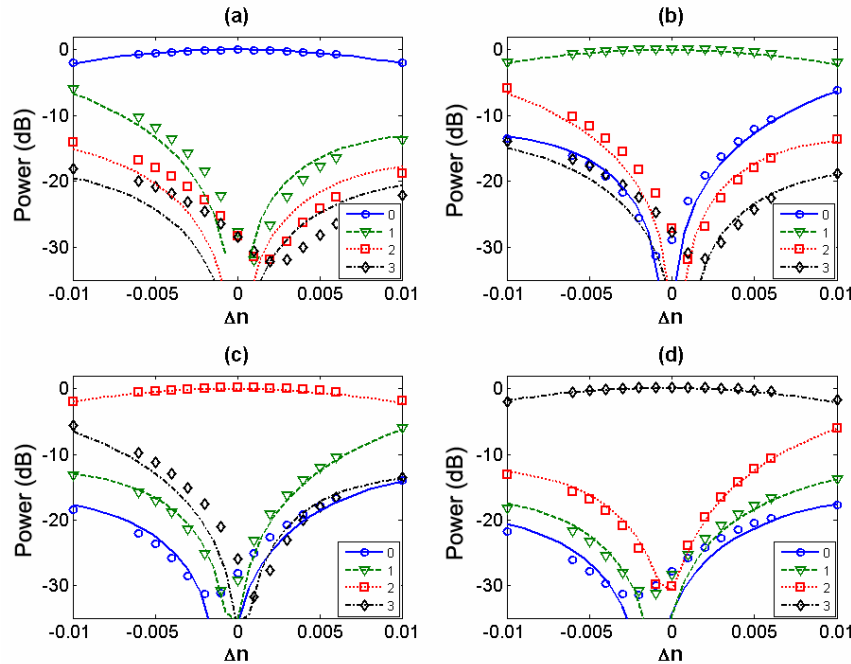


Fig. 6. The portions of the power of incident laser beam (TE mode) directed to the optical outputs 1 – 3 of the switch as functions of the mismatch, $\Delta n = n_2 - n_{2,m}$, between the actual refractive index of the liquid, n_2 , and the index, $n_{2,m}$, corresponding to the maximum of diffraction in m th order (as given by Eq. 1). Plots in (a) – (d) correspond to $m = 0 - 3$ (and the switch in the states 0 – 3), respectively. Power directed to the optical outputs 0 – 3 is plotted in blue, green, red, and black, respectively. Lines show results of numerical simulations obtained with multi-wave coupling analysis; symbols show results of numerical solutions of the wave equation.

perfectly shaped diffraction grating, this procedure is expected to provide inaccuracy on the order of 1×10^{-3} in the refractive index and a cross-talk of < -20 dB. Therefore, we believe that the relatively strong cross-talk (and low extinction ratio) in the switch was mostly due to imperfections in the shape of the diffraction grating. The imperfections included non-uniformity of the segment heights and roughness of the surface and were clearly visible under an optical microscope. The imperfections resulted from limited fidelity of the transfer of the relief of the commercial blazed grating onto the diffraction channel during the device fabrication.

The response time of the optofluidic switch, which is currently at 55 ms, can be shortened by increasing the driving pressure and by reducing the diameter of the diffraction channel (from current 4.5 mm to 1-2 mm, still sufficient for a 0.4 mm laser beam), thus reducing the amount of liquid that needs to be displaced from it at each switching. Further reduction of the response time, though at the expense of increased consumption of liquid during switching, can be achieved by increasing the depth of the channels, which would increase the speed of flow through the device at a given driving pressure.

In summary, a concept of $1 \times N$ optofluidic switches based on blazed diffraction gratings has been introduced and a 1×4 switch has been designed, fabricated, and tested. The switch

does not consume electric power or liquid in its steady states, has a response time of 55 ms, insertion loss of ~ 2.5 dB, cross-talk of -9.8 dB, and extinction ratio of 9.6 dB. The proposed $1 \times N$ optofluidic switches have an advantage of potentially simple integration with other microfluidic elements for lab-on-a-chip applications. Furthermore, the cross-talk and the extinction ratio in the present 1×4 switch are expected to be substantially improved by perfecting the shape of the diffraction grating, and the response time of the switch can be reduced by modifying the microfluidic channels.

Acknowledgments

We thank Virginia VanDelinder for useful suggestions. Partial support from the Defense Advanced Research Projects Agency's Center for Optofluidic Integration and National Science Foundation.